

1989000820

617981

14p.

55-46

~~165576~~140
April-June 1988

N89 - 10191

JPL

Australia 31-GHz Brightness Temperature Exceedance Statistics

B. L. Gary

Microwave Observational Systems Section

Water vapor radiometer measurements were made at DSS 43 during an 18-month period. Brightness temperatures at 31 GHz were subjected to a statistical analysis which included correction for the effects of occasional water on the radiometer radome. An exceedance plot has been constructed, and the 1 percent exceedance statistic occurs at 120 K. The 5 percent exceedance statistic occurs at 70 K, compared with 75 K in Spain. These values are valid for all of the three-month data groupings that were studied.

I. Observations

In [1], models were derived for weather effects on Ka-band performance analysis. To use the models, measurements of noise temperature effects of a measured amount of water vapor are needed. Therefore, the RO6 water vapor radiometer (WVR) was deployed at DSS 43 in Australia for several years prior to early 1986. Beginning in the spring of 1984, RO6 was pointed at an elevation angle of 45 degrees so that line-of-sight data would be less affected by water on the radome cover. Tip curve data were taken for approximately 30 minutes once or twice weekly. All remaining hours were devoted to 45-degree line-of-sight data.

A line-of-sight observation consists of a 15-minute average of sky count data for the 20.7- and 31.4-GHz radiometer channels and a recording of physical temperatures within RO6. Hot load and base load readings were made. Data were recorded on a diskette, which was replaced twice weekly and mailed to JPL. The operation of RO6 was conducted by DSS 43 station personnel.

RO6 data from the 18-month period of July 1984 through December 1985 are the subject of the present article. Data from earlier epochs are subject to uncertain effects due to water remaining on the radome after precipitation, because the WVR was pointed at zenith at these earlier times. As will be explained below, radome water corrections are a crucial part of obtaining exceedance statistics at the high brightness temperature regime, and these corrections are much greater (and are subject to much greater uncertainties) for zenith data than for 45-degree data. See [2] for Spain measurements.

II. Data Reduction

In order to convert radiometer sky counts to brightness temperature, it is necessary to know the gain of the radiometer channel that is being used. Tip curves enable this measurement of gain to be made when sky conditions are clear. When it is cloudy, tip curve gains are "noisy." Plots of gain versus instrument temperature were made for several data groupings. Figure 1 is a plot of this relationship for both channels, and it

represents data from the 6-month period of July to December 1984. The solid line was determined from data from August 1985. The agreement of the plotted points in Fig. 1 with the lines indicates that the gain-temperature relationships did not change over a 13-month interval.

The gain-temperature relationship represented by the straight line in Fig. 1(b) was used to reduce all 31-GHz data that will be described in this report

$$\text{Gain 2} = 8.340 - 0.206 (T_{\text{amb}} - 40^{\circ}\text{C})$$

where the units for gain are counts/ $^{\circ}\text{C}$.

Figure 2 is a sample output from a computer program that reduces raw data files and calculates sky brightness temperatures. The first three rows correspond to tip curves, and they yielded measurements of the gain and tip curve correlation coefficient (R-squared) for each channel. The column of interest in this figure is labeled " TB_{zen} ." For the line-of-sight data cycles, TB_{zen} is the zenith-normalized brightness temperature. There is an entry in this column every 15 minutes. The channel 2 entries in this column-pair are "input" for the next data-reducing program.

The next program collects the 31-GHz zenith-normalized brightness temperatures for a user-specified time period and creates a histogram. Figure 3 is a histogram for the entire 18-month period. The left-most four columns are zenith-normalized brightness temperatures. The fifth column is the number of occasions that a measurement has a given brightness temperature value (designated by the first four columns).

Figures 4(a) and (b) are exceedance plots of 3-month groupings of the data in the previous figure. The figure labels use the term *wet radome* to remind the reader that the plots are based on data that have not been corrected for water that may have been on the RO6 radome when data were taken.

III. Radome Water Correction Procedure

High brightness temperature values can be produced by water drops remaining on the radome after rain or overnight dew. The SCAMS (Scanning Microwave Spectrometer) WVR has been used to investigate radome water effects. SCAMS measures sky brightness temperature at zenith angles that range from 0 (zenith) to ± 60 degrees (i.e., a 30-degree elevation angle at opposite azimuths). After rain, the zenith brightness temperatures are affected the most because more water remains at the top of the curved radome than on the sides. Measurements from each of the SCAMS viewing directions can be used to infer zenith brightness temperature, which will be

referred to as TB_z (for TB zenith-normalized). When the radome is dry and when there are no lumpy clouds, each of these TB_z values are the same. When different amounts of water are standing on the various parts of the radome, however, there are different TB_z values. The smallest value corresponds to the driest part of the radome. When the radome has water, the lowest value for TB_z usually comes from one of the 60-degree zenith angle viewing directions.

It is fortunate for the present investigation that SCAMS was used at DSS 43 in Spain for a 4-month study of 31-GHz brightness temperature statistics. During the course of analysis of these data, some interesting things were discovered about the effect of water on the SCAMS radome. These findings play a crucial role in deriving a radome water-correcting algorithm for the RO6 Australia data. The Spain data are described in [2]. Some of the Spain data that will be presented here are taken from this article.

Figure 5 is a plot of TB_z that is derived from the zenith, -48 -degree, and -60 -degree zenith angle measurements made in Spain. The vertical scale is labeled in 10-K increments, and the horizontal scale is labeled in 1-hour increments. The highest trace invariably corresponds to the zenith data, meaning that there is always more water at the top of the radome than on the sides. The three traces are together before high- TB_z events, and they approach each other during a "drying-out" period. Note that during an event there can be disparities as great as 24 K. While it is raining, the traces are "noisy." During the drying-out phase, the traces are smooth but separated. The last event has a drying-out period that lasts 13 hours.

An empirical relationship has been deduced for the amount of TB_z excess (attributable to radome water) and the measured (uncorrected) TB_z . This relationship has been derived for the ± 48 -degree SCAMS data. Figure 6 is a plot of the data that have enabled this relationship to be determined. The curves can be used to derive corrections, which the following example will illustrate. When measured TB_z is 80 K, 50 percent of the time the required correction is 27 K, 5 percent of the time the correction is 16 K, and another 25 percent of the time the correction is 35 K. This plot could have been used to correct ± 48 -degree measurements of TB_z to derive dry-radome-equivalent TB statistics. For SCAMS it was not necessary to use this procedure, since SCAMS measured TB_z for many angles, and the lowest TB_z value was adopted as corresponding to "dry."

Table 1 was derived from the plot of Fig. 6. Note that more categories are used for the redistribution of TBs. The following example will illustrate the use of this table. If there are 100 entries in the histogram of observed (uncorrected) TB_z values at the 100-K level, 10 percent of these entries (i.e.,

10 entries) would be moved to the histogram location 18 K below 100 K (i.e., $100 - 18 = 82$ K), 15 percent would be moved to the histogram location 24 K below 100 K, etc.

Before the SCAMS algorithm is used for correcting radome water effects that are present in the RO6 (Australia) data, it is necessary to demonstrate that the two WVRs respond to rain in the same way. That is to say, whenever TB_z for SCAMS is too large by a certain amount due to radome water, is TB_z for RO6 too large by the same amount? The answer is yes, and this was established by conducting side-by-side tests with a garden hose simulation of rain.¹

IV. Corrected Brightness Temperature Statistics

Figure 7 is a histogram of the "corrected" brightness temperatures. As in Fig. 3, the first four columns are zenith brightness temperatures and the fifth column is the number of entries in the histogram bin-range.

Table 2 outlines exceedance statistics for the observed (uncorrected) and "radome-water-corrected" brightness temperature histograms. Columns 1 and 2 correspond to "zenith" and "30-degree elevation angle" brightness temperatures (excluding the 3-K cosmic background component). Column 3 is an exceedance table for the uncorrected data (in Fig. 3), and column 4 is an exceedance table for the corrected data (in Fig. 7). Columns 5 through 10 correspond to 3-month group-

ings of the uncorrected data. Columns 11 through 16 correspond to 3-month groupings of the corrected data.

Figures 8(a) and (b) are exceedance plots of the uncorrected and corrected TBs (columns 3 and 4 of Table 2). The difference between the plotted line and "▲" symbols shows the result of correcting for radome water effects. The difference is "substantial," which accounts for the long explanation presented (in the previous section) of what was involved in correcting measured TBs for the effects of radome water.

Figure 9 shows exceedance plots for the 3-month groupings of corrected TB data. It is noteworthy that the exceedance statistics do not change with season in the 1 percent region.

The Spain exceedance statistics are shown in the next two figures. Figure 10 is for the 4-month observing period March to June 1984. (Remember that all Spain data shown here would correspond to "dry" even though the correcting table described above was not employed in reducing the Spain data.) The several lines correspond to different data-averaging times. The Australia data have an averaging time of 15 minutes per data point, so that is the appropriate time to use in selecting an exceedance trace in this figure. Figure 11 is based on the data in the previous figure, and it reflects an adjustment that was made for the difference in rainfall that occurred during the 4-month observing period and the climatic average for Madrid. This adjustment is described in the Spain exceedance statistic report [2].

Figure 12 is a repeat of Fig. 9, except that the Spain data of the previous figure are plotted for comparison. There is a remarkable similarity in the levels of the exceedance plots from both stations.

¹B. L. Gary, "Rain on Radome Effects," internal memorandum, Jet Propulsion Laboratory, Pasadena, California, November 3, 1985.

References

- [1] S. D. Slobin, "Models of Weather Effects on Noise Temperature and Attenuation for Ka- and X-Band Telemetry Performance Analysis," *TDA Progress Report 42-88*, vol. October-December 1986, Jet Propulsion Laboratory, Pasadena, California, pp. 135-140, February 15, 1987.
- [2] B. L. Gary, "Spain 31-GHz Brightness Temperature Exceedance Statistics," *TDA Progress Report 42-94*, vol. April-June 1988, Jet Propulsion Laboratory, Pasadena, California, August 15, 1988 (this issue).

Table 1. Correction table for radome water effects (corrections to brightness temperature versus uncorrected brightness temperature)

TB_z	Redistribution percentages					
	10	15	25	25	15	10
25	0	0	0	0	0	0
30	0	0	1	3	4	6
40	3	6	9	11	13	15
50	7	9	13	17	21	23
70	11	17	22	26	30	36
100	18	24	29	33	38	44
140	24	30	35	39	45	51
200	31	37	42	46	54	60
220	33	39	44	48	56	63

Table 2. Exceedance table for 18-months of 31-GHz brightness temperature data at DSS-43

TB	TB ₃₀	All wet	All dry	4JASW	4ONDW	5JFMW	5AMJW	5JASW	5ONDW	4JASD	4ONDD	5JFMD	5AMJD	5JASD	5ONDD
		%>	%>												
10.0	14.0	98.8	98.8	98.2	97.6	99.9	98.7	99.9	100.0	98.2	97.6	98.6	98.6	99.0	99.2
11.0	15.9	96.4	96.2	93.7	94.9	99.2	96.5	98.2	98.5	93.5	94.8	96.6	96.6	97.0	97.3
12.0	17.9	91.1	90.8	83.2	89.9	96.8	91.6	85.6	96.4	82.8	89.6	92.6	92.2	90.2	91.3
13.0	19.9	84.2	83.5	70.8	83.3	94.1	83.2	68.3	91.6	70.0	82.8	87.4	85.7	80.5	82.5
14.0	21.8	76.6	75.7	60.0	75.7	90.7	75.6	51.1	84.1	58.9	75.0	81.3	79.1	70.6	73.1
15.0	23.7	68.8	67.5	50.7	67.8	86.0	66.1	41.2	75.2	49.4	66.9	74.5	71.2	62.1	64.5
16.0	25.7	60.2	58.6	43.1	58.7	79.3	56.4	34.8	64.8	41.6	57.5	66.0	62.2	53.8	55.7
17.0	27.6	52.7	50.8	37.9	50.8	73.0	47.1	30.7	54.0	36.2	49.3	58.5	53.9	46.8	47.9
18.0	29.5	46.6	44.4	34.2	44.8	65.8	40.0	27.6	45.9	32.4	43.2	51.6	46.9	40.9	41.5
19.0	31.4	40.8	38.4	30.6	39.2	58.2	33.8	24.8	39.1	28.7	37.3	44.8	40.3	35.3	35.7
20.0	33.3	35.3	32.7	27.8	34.2	49.1	29.4	23.1	33.0	25.9	32.2	37.6	34.1	30.4	30.5
22.0	37.1	27.0	24.1	23.8	26.4	34.2	23.5	20.7	25.3	21.7	24.1	26.2	24.5	23.0	23.0
24.0	40.8	21.7	18.0	19.9	22.0	24.1	19.7	18.7	21.2	17.3	19.0	18.3	18.0	17.6	17.7
26.0	44.6	18.5	15.0	17.8	19.6	17.8	17.4	17.2	18.6	15.1	16.3	14.8	14.9	14.9	15.0
28.0	48.3	16.2	12.2	16.0	17.9	13.9	16.2	15.9	16.7	12.7	13.1	11.6	12.1	12.1	12.3
30.0	51.9	14.7	9.9	14.9	16.5	11.5	15.2	14.9	15.3	10.8	10.4	9.0	9.7	9.8	10.0
32.0	55.6	13.3	8.2	13.9	15.0	9.7	14.1	13.8	14.1	9.3	8.3	7.2	7.9	8.1	8.3
34.0	59.2	12.1	7.1	12.9	13.0	8.8	13.3	12.6	12.9	8.2	7.0	6.0	6.7	6.9	7.1
36.0	62.7	11.2	6.2	12.0	11.9	8.0	12.6	11.5	12.1	7.3	6.0	5.2	5.8	5.9	6.2
38.0	66.3	10.2	5.4	11.3	10.4	7.2	11.9	10.4	11.1	6.4	5.2	4.5	5.0	5.1	5.3
40.0	69.8	9.4	4.8	10.7	9.5	6.5	10.9	9.6	10.3	5.7	4.6	3.9	4.4	4.5	4.7
42.0	73.3	8.6	4.2	9.9	8.6	5.7	10.1	8.9	9.5	5.0	4.0	3.4	3.8	3.9	4.1
44.0	76.8	7.9	3.8	9.2	7.7	5.2	9.5	8.2	9.0	4.6	3.6	3.1	3.4	3.5	3.6
46.0	80.2	7.3	3.3	8.7	7.2	4.5	8.7	7.5	8.3	4.0	3.2	2.7	3.0	3.0	3.2
48.0	83.6	6.8	3.0	8.1	6.7	4.1	8.0	7.0	7.7	3.6	2.9	2.5	2.8	2.8	2.9
50.0	87.0	6.3	2.7	7.6	6.1	3.8	7.0	6.4	7.3	3.2	2.6	2.3	2.5	2.5	2.6
55.0	95.3	5.2	2.2	6.5	4.8	3.0	5.3	5.4	5.9	2.5	2.1	1.9	2.0	1.9	2.1
60.0	103.4	4.2	1.8	5.2	4.1	2.4	4.5	4.2	4.7	2.0	1.7	1.6	1.6	1.6	1.7
65.0	111.3	3.5	1.4	4.4	3.5	2.1	3.8	3.2	3.8	1.5	1.4	1.3	1.3	1.2	1.3
70.0	119.1	3.0	1.1	3.6	2.9	1.8	3.1	2.5	3.3	1.1	1.1	1.1	1.1	1.0	1.1
75.0	126.6	2.5	0.9	3.0	2.4	1.7	2.5	2.1	2.8	0.9	0.9	0.9	0.9	0.9	0.9
80.0	134.0	2.1	0.8	2.5	2.1	1.4	2.0	1.7	2.3	0.7	0.8	0.8	0.8	0.7	0.8
85.0	141.2	1.8	0.6	2.1	1.8	1.2	1.6	1.4	2.0	0.5	0.7	0.7	0.7	0.6	0.7
90.0	148.3	1.5	0.5	1.7	1.5	1.2	1.2	1.2	1.7	0.4	0.6	0.6	0.6	0.5	0.6
95.0	155.1	1.3	0.5	1.4	1.2	1.1	1.0	0.9	1.4	0.3	0.5	0.6	0.5	0.5	0.5
100.0	161.8	1.1	0.4	1.1	1.0	1.0	0.8	0.8	1.2	0.3	0.4	0.5	0.4	0.4	0.4
110.0	174.5	0.8	0.3	0.7	0.8	0.8	0.5	0.6	0.8	0.1	0.3	0.4	0.3	0.3	0.3
120.0	186.6	0.6	0.2	0.5	0.6	0.7	0.4	0.4	0.6	0.1	0.2	0.3	0.2	0.2	0.2
130.0	197.9	0.4	0.1	0.3	0.5	0.6	0.2	0.3	0.4	0.0	0.1	0.2	0.2	0.2	0.2
140.0	208.5	0.3	0.1	0.2	0.3	0.5	0.1	0.2	0.4	0.0	0.1	0.1	0.1	0.1	0.2
150.0	218.3	0.2	0.1	0.1	0.3	0.4	0.1	0.2	0.2	0.0	0.0	0.1	0.1	0.1	0.1
160.0	227.5	0.2	0.0	0.0	0.2	0.3	0.0	0.1	0.2	0.0	0.0	0.1	0.1	0.1	0.1
170.0	235.8	0.1	0.0	0.0	0.1	0.3	0.0	0.1	0.1	0.0	0.0	0.0	0.0	0.0	0.0
180.0	243.5	0.1	0.0	0.0	0.1	0.2	0.0	0.0	0.1	0.0	0.0	0.0	0.0	0.0	0.0
190.0	250.4	0.1	0.0	0.0	0.0	0.2	0.0	0.0	0.0	0.0	0.0	0.0	0.0	0.0	0.0
200.0	256.6	0.0	0.0	0.0	0.0	0.0	0.0	0.0	0.0	0.0	0.0	0.0	0.0	0.0	0.0

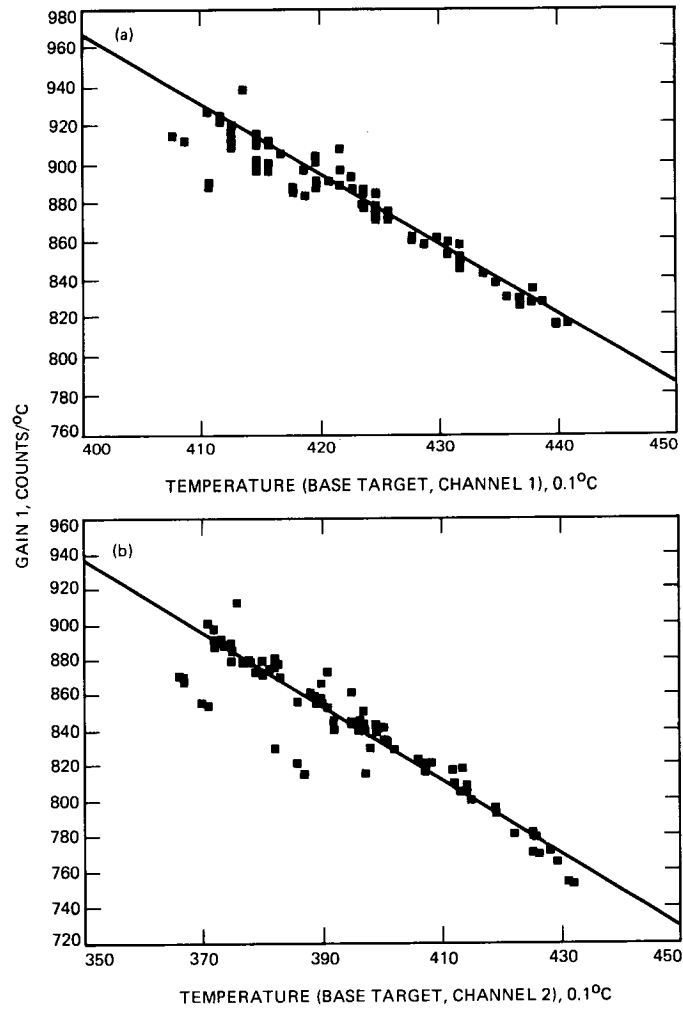


Fig. 1. WVR instrument gain versus mixer temperature from tip curves during a 6-month period in 1984. The straight line is based on data from August 1985.

01-10-1987 10:24:57 B:A5306.DAT to A:A5306.001
J-range = 2 to 14 TB' REJECT CRITERION= 100 degK

WILL DO TIP REDUCTION

NOTE: TIP data has entries up to TBzen columns; line-of-sight data has dots in some columns, & TBobs'd is for 45 deg elev'n

DAY	HR	MN	..TEMPS..	..GAINS...	..TB obs'd..	..R**2...	...RMS...	RJ	VAP	LIQ	..TBzen..	..good.tip.data..	G(t)
306	2	57	43.6 42.2	8.35 7.84	21.9 15.7	1.00 0.99	0.67 0.62	11	1.47	-26	21.9 15.7	43.6 8.35 42.2 7.84	835 789
306	3	2	43.6 42.2	8.38 7.87	22.8 16.4	1.00 1.00	0.61 0.52	00	1.55	-20	22.8 16.4	43.6 8.38 42.2 7.87	835 788
306	3	8	43.5 42.1	8.39 7.88	22.8 16.7	1.00 1.00	0.53 0.47	00	1.54	-11	22.8 16.7	43.5 8.39 42.1 7.88	841 789
306	3	20	43.7 42.2	30.1 23.3	0.32 0.29	00	1.45	25	22.5 17.5	834 787
306	3	35	43.6 42.3	31.1 23.2	0.25 0.20	00	1.54	9	23.2 17.4	835 785
306	3	50	43.7 42.3	31.5 23.9	0.22 0.13	00	1.55	22	23.5 18.0	834 785
306	4	5	43.7 42.4	30.9 23.7	0.13 0.06	00	1.50	24	23.0 17.8	832 784
306	4	20	43.7 42.3	31.3 23.7	0.30 0.27	00	1.54	18	23.3 17.8	834 784
306	4	35	43.7 42.3	31.3 23.6	0.17 0.08	00	1.54	17	23.3 17.7	834 786
306	4	50	43.7 42.3	31.7 23.8	0.24 0.18	00	1.57	17	23.6 17.9	834 785
306	5	5	43.6 42.2	32.8 24.2	0.16 0.14	00	1.64	14	24.4 18.2	835 787
306	5	20	43.5 42.1	33.8 24.4	0.20 0.21	00	1.72	6	25.1 18.3	839 788
306	5	35	43.5 42.1	33.6 24.2	0.19 0.35	00	1.71	3	25.0 18.2	839 790
306	5	50	43.6 42.1	33.0 24.6	0.47 0.39	00	1.65	21	24.6 18.5	835 790
306	6	5	43.7 42.2	35.1 25.2	2.39 1.39	00	1.81	8	26.1 18.9	834 788
306	6	20	43.4 42.0	39.6 27.1	0.35 0.30	00	2.13	-4	29.4 20.3	842 791
306	6	35	43.4 42.0	37.3 25.3	0.72 0.82	00	1.99	-19	27.7 18.9	842 792
306	6	50	43.4 41.7	35.8 23.5	0.53 0.71	00	1.92	-42	26.6 17.7	844 798
306	7	5	43.2 41.4	36.2 23.0	0.20 0.37	00	1.98	-61	26.9 17.3	850 804
306	7	20	43.0 41.1	38.1 24.3	0.23 0.21	00	2.10	-53	28.3 18.3	857 811
306	7	35	42.9 40.9	37.2 24.0	0.86 0.69	00	2.03	-49	27.6 18.0	861 815
306	7	50	42.8 40.5	37.1 24.3	0.38 0.47	00	2.01	-41	27.6 18.2	867 823
306	8	5	42.5 40.1	39.0 24.2	0.38 0.43	00	2.18	-68	29.0 18.2	878 830
306	8	20	42.3 39.8	40.2 26.9	0.31 0.67	00	2.19	-16	29.8 20.1	883 837
306	8	35	42.3 39.6	39.1 27.2	0.64 1.10	00	2.08	6	29.1 20.4	884 841
306	8	50	42.2 39.5	40.2 28.5	0.52 1.37	00	2.13	24	29.8 21.3	888 844
306	9	5	42.2 39.3	41.0 31.5	0.30 0.78	00	2.09	90	30.4 23.5	888 846
306	9	20	42.1 39.2	42.0 31.7	0.36 0.82	00	2.18	81	31.2 23.6	891 848
306	9	35	42.1 39.1	42.0 33.9	0.97 1.94	00	2.10	137	31.2 25.2	892 851
306	9	50	42.2 39.2	38.4 29.6	0.64 1.45	00	1.93	75	28.5 22.1	888 849
306	10	5	42.2 39.3	38.0 27.1	0.50 0.95	00	1.99	17	28.2 20.3	888 848
306	10	20	42.2 39.2	38.9 28.5	0.20 0.39	00	2.02	39	28.9 21.3	890 848
306	10	35	42.2 39.3	38.0 29.0	0.48 0.88	00	1.92	65	28.2 21.6	887 848
306	10	50	42.2 39.2	38.2 28.0	0.40 0.78	00	1.98	37	28.4 20.9	888 849
306	11	5	42.1 39.1	38.7 27.3	0.23 0.62	00	2.04	13	28.7 20.4	893 851
306	11	20	42.2 39.2	38.2 27.5	0.29 0.53	00	1.99	25	28.3 20.5	888 850
306	11	35	42.2 39.2	39.6 29.8	0.46 1.00	00	2.04	64	29.4 22.2	890 850
306	11	50	42.2 39.2	37.6 26.2	0.58 1.15	00	1.99	-1	28.0 19.6	888 850
306	12	5	42.2 39.2	38.0 27.1	0.91 1.90	00	1.99	18	28.2 20.3	890 849
306	12	20	42.2 39.2	40.4 33.8	0.73 1.59	00	1.95	155	30.0 25.1	887 848
306	12	35	42.2 39.2	40.3 32.0	0.59 1.21	00	2.02	109	30.0 23.8	888 848
306	12	50	42.2 39.3	39.2 29.2	0.65 1.26	00	2.02	54	29.1 21.8	887 847
306	13	5	42.3 39.3	40.1 33.2	1.18 2.50	00	1.96	144	29.8 24.7	883 846
306	13	20	42.3 39.4	43.3 39.2	1.24 2.95	00	2.01	258	32.1 29.1	885 845
306	13	35	42.3 39.3	42.3 38.8	0.91 1.78	00	1.94	261	31.4 28.8	885 846
306	13	50	42.2 39.3	40.6 35.2	0.66 1.40	00	1.92	189	30.1 26.1	887 846
306	14	5	42.2 39.3	39.7 33.7	0.99 2.05	00	1.90	163	29.5 25.1	887 847
306	14	20	42.2 39.3	40.8 34.4	1.04 2.24	00	1.96	168	30.3 25.6	890 847
306	14	35	42.2 39.3	40.8 35.3	1.00 2.02	00	1.94	188	30.3 26.2	888 847
306	14	50	42.2 39.3	39.6 33.2	0.29 0.59	00	1.91	150	29.4 24.7	888 847
306	15	5	42.1 39.2	41.0 34.8	0.67 1.38	00	1.97	174	30.5 25.9	891 849
306	15	20	42.2 39.3	38.4 32.0	0.43 0.72	00	1.84	138	28.5 23.9	887 848
306	15	35	42.2 39.2	39.4 34.1	0.50 1.01	00	1.85	177	29.2 25.4	888 848
306	15	50	42.1 39.2	40.5 35.3	0.24 0.37	00	1.91	195	30.1 26.3	892 850
306	16	5	42.2 39.2	39.3 34.2	0.42 0.90	00	1.84	181	29.2 25.4	890 850
306	16	20	42.2 39.2	38.0 32.7	0.38 0.80	00	1.79	159	28.3 24.4	888 850
306	16	35	42.2 39.2	37.7 31.1	0.98 1.91	00	1.82	123	28.0 23.2	890 850
306	16	50	42.2 39.2	38.7 33.4	0.65 1.32	00	1.83	167	28.8 24.8	890 849
306	17	5	42.2 39.2	39.2 34.3	0.51 1.03	00	1.84	183	29.1 25.5	890 850
306	17	20	42.3 39.2	37.4 33.1	0.64 1.39	00	1.72	178	27.8 24.7	885 848
306	17	35	42.2 39.2	38.1 32.5	0.80 1.48	00	1.80	154	28.3 24.2	888 849
306	17	50	42.1 39.2	38.0 31.6	0.17 0.34	00	1.83	130	28.2 23.5	891 849
306	18	5	42.2 39.2	37.6 31.8	0.67 1.45	00	1.78	142	27.9 23.7	888 848
306	18	20	42.3 39.3	36.6 31.3	0.82 1.70	00	1.72	142	27.2 23.3	885 847
306	18	35	42.2 39.2	36.9 29.8	0.30 0.56	00	1.80	99	27.4 22.2	888 848
306	18	50	42.2 39.2	37.8 32.3	0.55 1.06	00	1.79	151	28.1 24.0	887 848
306	19	5	42.2 39.2	39.0 34.1	0.39 0.71	00	1.83	181	29.0 25.3	888 848
306	19	20	42.2 39.3	39.3 33.0	0.64 1.29	00	1.89	150	29.2 24.6	890 847

Fig. 2. Sample output from a computer program that reduces raw data

18-MONTH UNCORRECTED (WET) 31-GHz BRIGHTNESS TEMPERATURE HISTOGRAM

	>140	100	:***		
137	138	139	140	12	:
133	134	135	136	12	:
129	130	131	132	10	:
125	126	127	128	18	:
121	122	123	124	19	:
117	118	119	120	20	:
113	114	115	116	29	:*
109	110	111	112	26	:
105	106	107	108	29	:*
101	102	103	104	42	:*
97	98	99	100	46	:*
93	94	95	96	51	:*
89	90	91	92	62	:**
85	86	87	88	77	:**
81	82	83	84	64	:**
77	78	79	80	82	:**
73	74	75	76	119	:****
69	70	71	72	112	:****
65	66	67	68	139	:*****
61	62	63	64	161	:*****
	58	59	60	148	:*****
	55	56	57	212	:*****
	52	53	54	170	:*****
	49	50	51	234	:*****
	46	47	48	242	:*****
	43	44	45	283	:*****
	40	41	42	359	:*****
		38	39	256	:*****
		36	37	272	:*****
		34	35	311	:*****
		32	33	410	:*****
		30	31	414	:*****
		28	29	547	:*****
		26	27	747	:*****
		24	25	1248	:*****
		22	23	1988	:*****
		20	21	2941	:*****
			19	1696	:*****
			18	1810	:*****
			17	2210	:*****
			16	2508	:*****
			15	2311	:*****
			14	2221	:*****
			13	2047	:*****
			12	1541	:*****
			11	732	:*****
			10	183	:*****
			<10	159	:*****

TOTAL # = 29430

NOTE: Above temperatures include 3°K cosmic background

Fig. 3. Histogram of zenith-normalized 31-GHz brightness temperature for an 18-month period. Data are not corrected for water-on-radome effects.

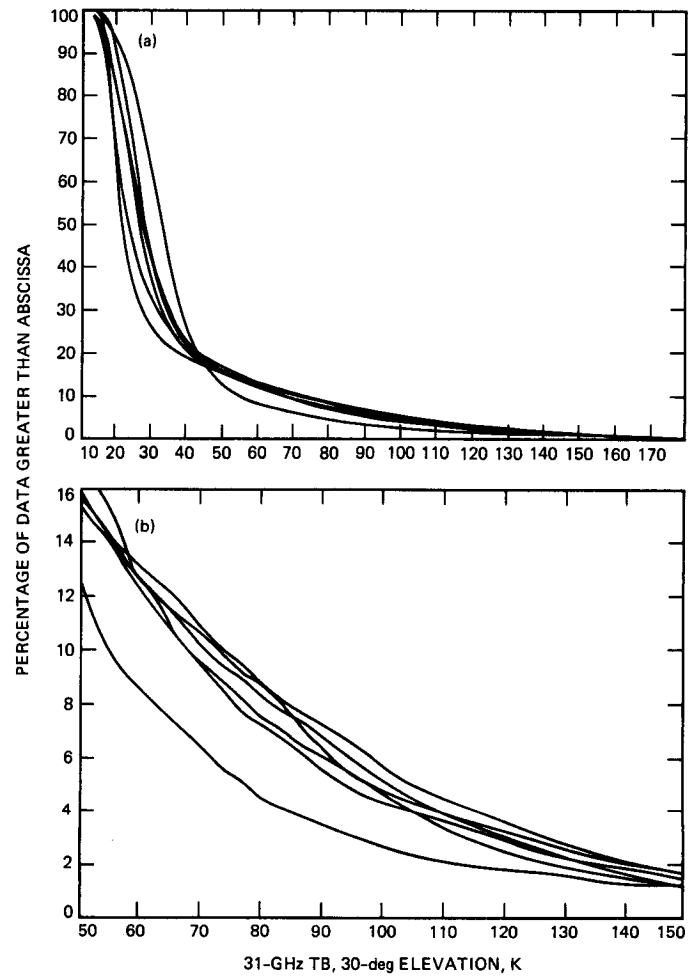


Fig. 4. Exceedance plots for 3-month groupings of 18 months' worth of 31-GHz zenith-normalized sky brightness temperature. Data are not corrected for water-on-radome effects.

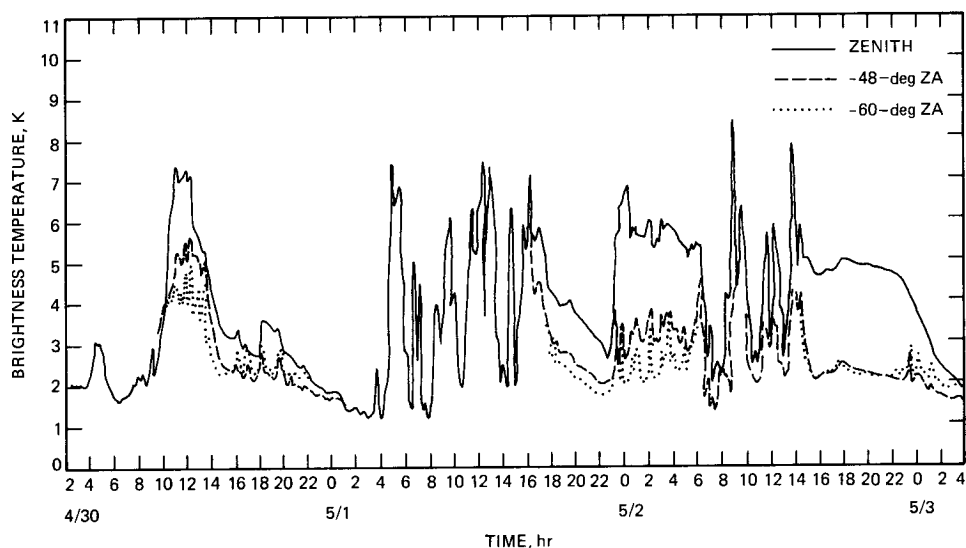


Fig. 5. Antenna temperature versus time for the elevation angles -60 degrees, -48 degrees, and zenith. The off-zenith data are normalized to zenith and are approximately the same when the radome is dry. Differences between these traces exist when water is on the radome.

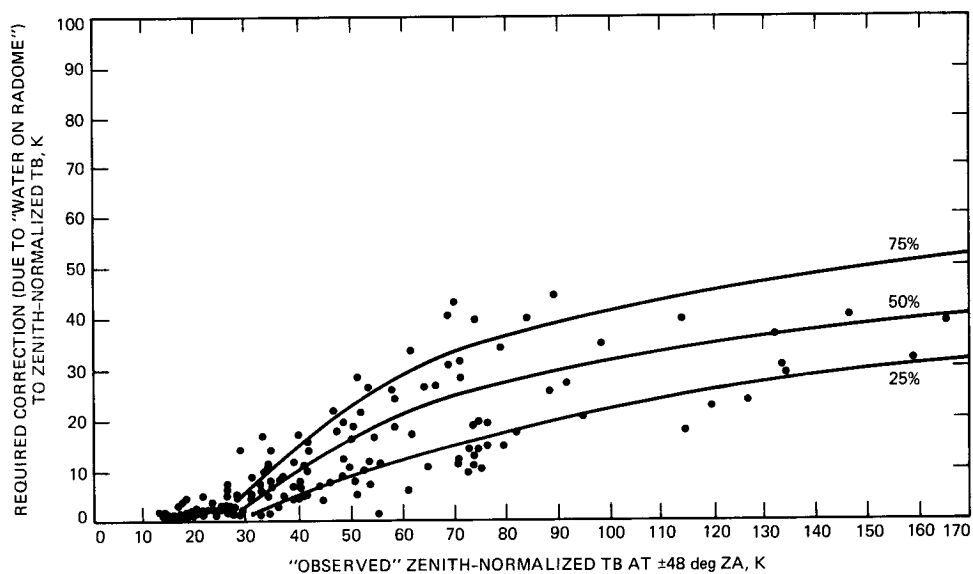


Fig. 6. An empirical relationship between observed zenith-normalized sky brightness temperature (X-coordinate) and the component of zenith-normalized sky brightness temperature that is due to water on the radome (Y-coordinate). Lines are hand-fit percentile estimators.

18-MONTH CORRECTED (DRY RADOME) 31-GHz BRIGHTNESS TEMPERATURE HISTOGRAM

	>140	24	:
137	138	139	140
133	134	135	136
129	130	131	132
125	126	127	128
121	122	123	124
117	118	119	120
113	114	115	116
109	110	111	112
105	106	107	108
101	102	103	104
97	98	99	100
93	94	95	96
89	90	91	92
85	86	87	88
81	82	83	84
77	78	79	80
73	74	75	76
69	70	71	72
65	66	67	68
61	62	63	64
	58	59	60
	55	56	57
	52	53	54
	49	50	51
	46	47	48
	43	44	45
	40	41	42
		38	39
		36	37
		34	35
		32	33
		30	31
		28	29
		26	27
		24	25
		22	23
		20	21
			19
			18
			17
			16
			15
			14
			13
			12
			11
			10
			<10

TOTAL # = 28299

NOTE: Above temperatures include 3°K cosmic background

Fig. 7. Histogram of wet-radome-corrected zenith sky brightness temperature for an 18-month period

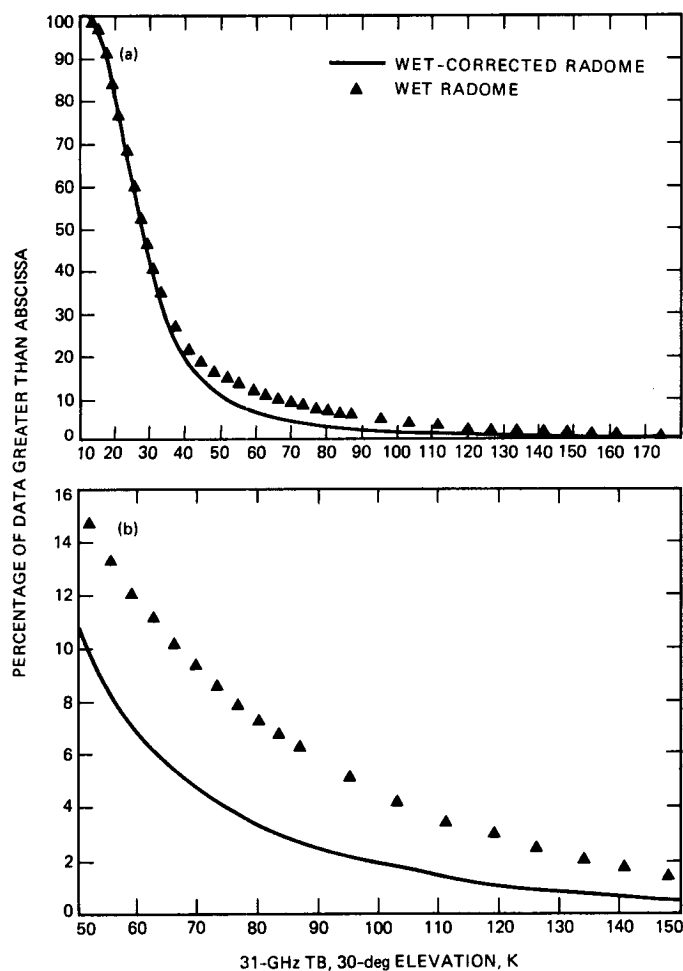


Fig. 8. The 31-GHz exceedance plots for 30-degree elevation for wet-radome data (Δ) and wet-radome-corrected data (lines)

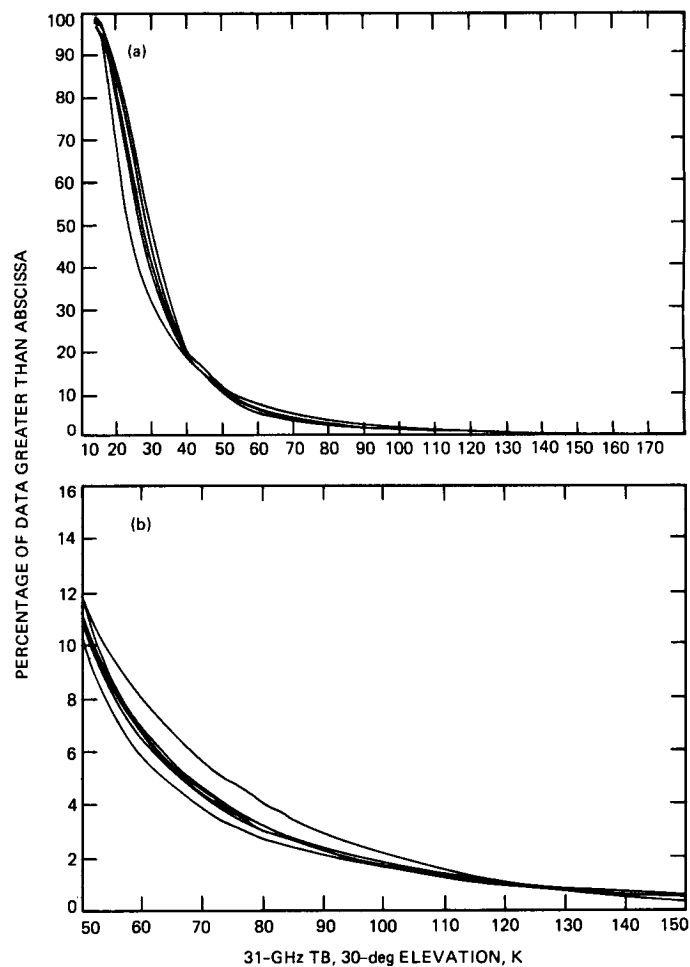


Fig. 9. The 31-GHz exceedance plots for 30-degree elevation for wet-radome-corrected-only data, grouped by season

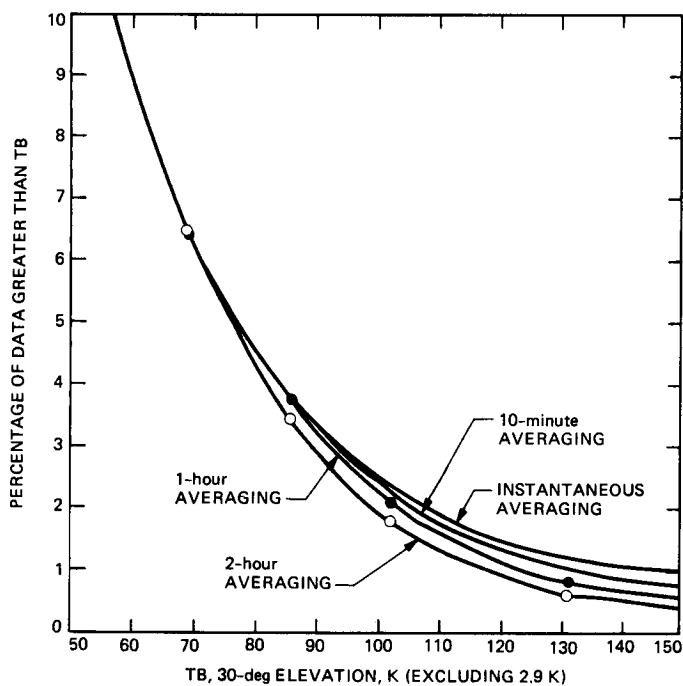


Fig. 10. Spain exceedance statistics [2]. Wet radome effects have been removed. Data are for a 4-month period in 1984 and are based on measurements from DSS 63.

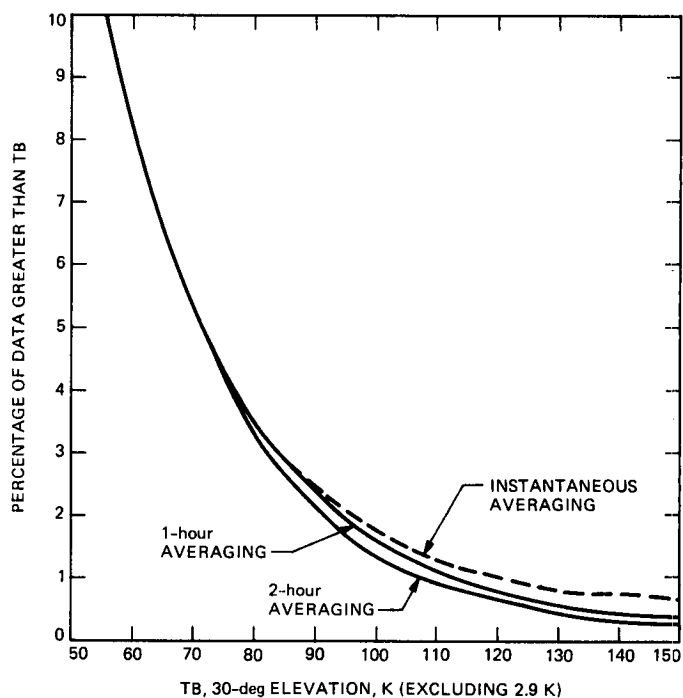


Fig. 11. Spain exceedance statistics with an adjustment made to correct for the larger-than-typical rainfall that occurred during the 4-month observing period in Spain (based on SCAMS WVR measurements)

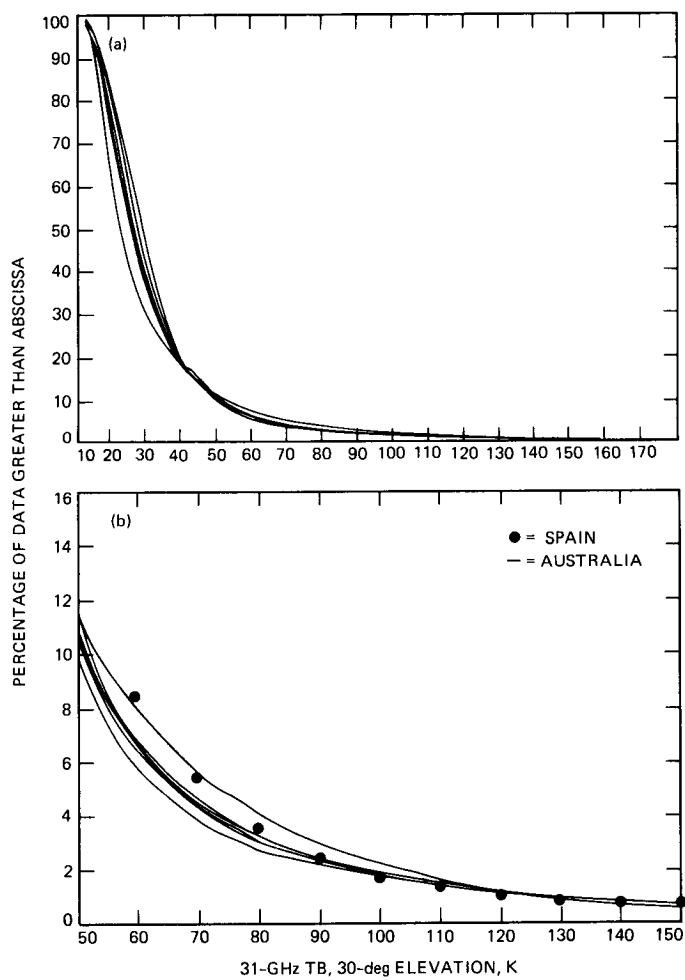


Fig. 12. Combination of Fig. 9 and Fig. 11 showing the similarity in exceedance plots for Spain and Australia